AD-A070 745 MICHIGAN TECHNOLOGICAL UNIV HOUGHTON DEPT OF METALLU--ETC F/G 11/6
FRACTURE TOUGHNESS OF WIDMANSTATTEN COLONIES OF AN ALPHA-BETA T--ETC(U)
JUN 79 K S CHAN, D A KOSS N00014-76-C-0037
UNCLASSIFIED TR-9 NL

END
DATE FILMED
8-79
DDC

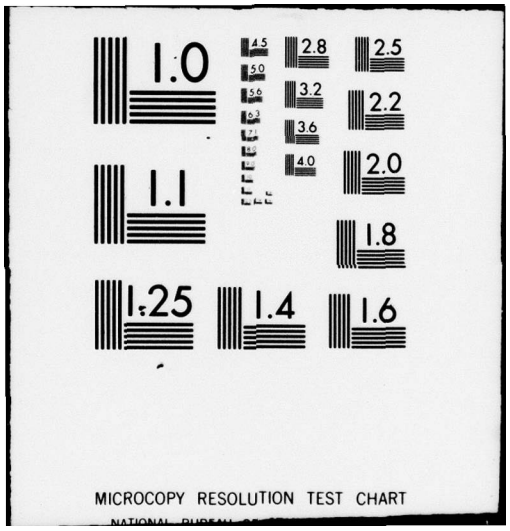
1.0
1.1
1.25
1.4
1.6
1.8
2.0
2.2
2.5
2.8
3.2
3.6
4.0
4.5
5.0
5.6
6.3
MICROCOPY RESOLUTION TEST CHART

TECHNICAL REPORT No. 9

To

THE OFFICE OF NAVAL RESEARCH

CONTRACT No. N00014-76-C-0037

LEVEL

FRACTURE TOUGHNESS OF WIDMANSTATTEN COLONIES OF AN ALPHA-BETA TITANIUM ALLOY

BY

K. S. CHAN AND D. A. KOSS

DEPARTMENT OF METALLURGICAL ENGINEERING

MICHIGAN TECHNOLOGICAL UNIVERSITY

HOUGHTON, MICHIGAN U.S.A.

FRACTURE TOUGHNESS OF WIDMANSTATTEN COLONIES OF AN α-β Ti ALLOY

by

K. S. Chan and D. A. Koss

Department of Metallurgical Engineering
Michigan Technological University
Houghton, Michigan 49931

Abstract

The fracture toughness behavior of individual α+β Widmanstatten colonies of the Ti-8Al-1Mo-1V alloy in the form of sheet has been investigated. Crack extension occurs predominantly across the α-β lamellae under conditions of plane stress and on planes which are inclined both to the thickness and the width of specimens. Polycrystalline material has also been examined and is observed to exhibit fracture along a plane inclined through the thickness but not inclined across the width. Crack-tip plasticity in both types of material is dominated by through-thickness deformation involving slip and often twinning. In the single colony specimens, the crack-tip plasticity has been characterized experimentally by identifying the active slip/twinning planes and by calculating the distribution of shear stresses on the possible deformation systems, using a maximum, macroscopic shear stress criteria. As suggested by the fracture behavior of the polycrystalline specimens, the macroscopic fracture plane across individual colonies is near that slip or twinning plane which experiences the largest shear stress when the macroscopic shear stress is a maximum. The plane stress fracture toughness of individual colonies depends strongly on colony orientation and also on the nature of the deformation at the crack-tip. High toughness of a colony is associated with multiple slip and twinning and with the absence of low energy fracture along or near interfaces, such as twin boundaries or α-β interfaces. Conversely, slip localization into coarse, inhomogeneous basal slip bands results in the crack extension along such bands

and in the lowest fracture toughness observed. Such fracture behavior can be readily understood in terms of an elastic-plastic model for crack advance along slip bands co-planar with a crack.

INTRODUCTION

Because of the hcp crystal structure of the α-phase, most α-β Ti alloys exhibit a considerable anisotropy of their mechanical properties when the α-phase is strongly textured; for a review, see ref. 1. Several studies show that texture can affect the fracture behavior of α-β Ti alloys.[2-6] In particular, the recent studies by Bowen[5] and Tchorzewski and Hutchinson[6] examine the anisotropy of the fracture toughness in textured Ti-6Aℓ-4V alloy plate with a relatively equiaxed α-β morphology. Both of these investigations observe that texture affects the toughness values and conclude that slip at the crack tip, which is dominated by the slip behavior of the hcp α-phase, is an important factor in determining the magnitude of the fracture toughness. Other studies have shown that the morphology of the α and β phases can also affect the fracture toughness of α-β Ti alloys with a Widmanstatten microstructure consisting of α and β platelets possessing superior toughness to that of an equiaxed α-β morphology.[7-14] This enhanced toughness has been associated with the ability of the acicular microstructure to influence the crack path, causing crack deflection. The resulting fracture path is tortuous and consists of significant amounts of cracking across the colonies on preferred planes within the α-phase.[11,12,14] In near-α Ti alloys, the degree of acicularity of the α and β phases can be quite high, and the microstructure often consists of relatively large colonies of aligned α and β platelets. While certain aspects of the fracture of these Widmanstatten microstructures are understood, the mechanisms controlling cracking across individual α-β colonies remain unclear. The purpose of this research is to examine the relationship between fracture toughness and crack-tip deformation behavior in individual Widmanstatten colonies of the near-α alloy, Ti-8Aℓ-1Mo-1V. While the test conditions are necessarily those which result in a state of plane stress at the crack-tip, certain qualitative extensions of the present conclusions to the case of plane strain are possible.

EXPERIMENTAL PROCEDURE

Large Widmanstatten colonies of the Ti-8Al-1Mo-1V alloy were grown by a β-anneal and slow, unidirectional cool technique developed by Wojcik.[15] It should immediately be noted that this technique is best suited for sheet material. Strips of the alloy in sheet form (1.65mm thick) were subjected to two consecutive passes at 23mm/hr and at 16mm/hr through an inductively heated hot zone at 1450-1500°C using a Ta susceptor. The process was performed in a dynamic vacuum of $<6.7 \times 10^{-4}$ Pa. For a strip of material 12mm wide x 230mm long, the yield per strip is one or two large α-β colonies, roughly 6mm wide x 10mm long and through the sheet thickness. Specimens were machined according to Fig. 1 with the largest colony located in the central portion of the gauge length. Shape changes which occur during the growth of the large colonies resulted in sheet which was no longer flat. Following Wojcik's procedures,[15] the specimen blanks were creep flattened in a dynamic vacuum of $<4 \times 10^{-4}$ Pa at a compressive stress of 6.6×10^{5} Pa at 680°C for one hour. The composition of a typical colony specimen was (in wt. %): Ti-7.6Al-1.0Mo-1.0V. Interstitial content (wt. ppm) was: 1160 oxygen, 170 nitrogen, 210 carbon, and 18 hydrogen.

After electropolishing gauge section at -35°C in a solution of perchloric acid, methyl alcohol, and n-butyl alcohol, the samples were single edge notched. Fatigue pre-cracking to a crack length shown in Fig. 1 was performed after an annealing treatment consisting of 760°C for 2 hours in a dynamic vacuum of $<3 \times 10^{-4}$ Pa followed by helium gas quenching. The resulting microstructure is illustrated in Fig. 2a and consists of about 90% α and 10% β in relatively well aligned, alternating lamellae of the α and β phases. Under these conditions, α_2 precipitates are not expected to form,[16] but the "interface phase," which forms as a layer between the α and β phases, is expected to be present.[17]

Polycrystalline specimens possessing a similar microstructure to the one described above were prepared by annealing in the β range for one hour at 1100°C

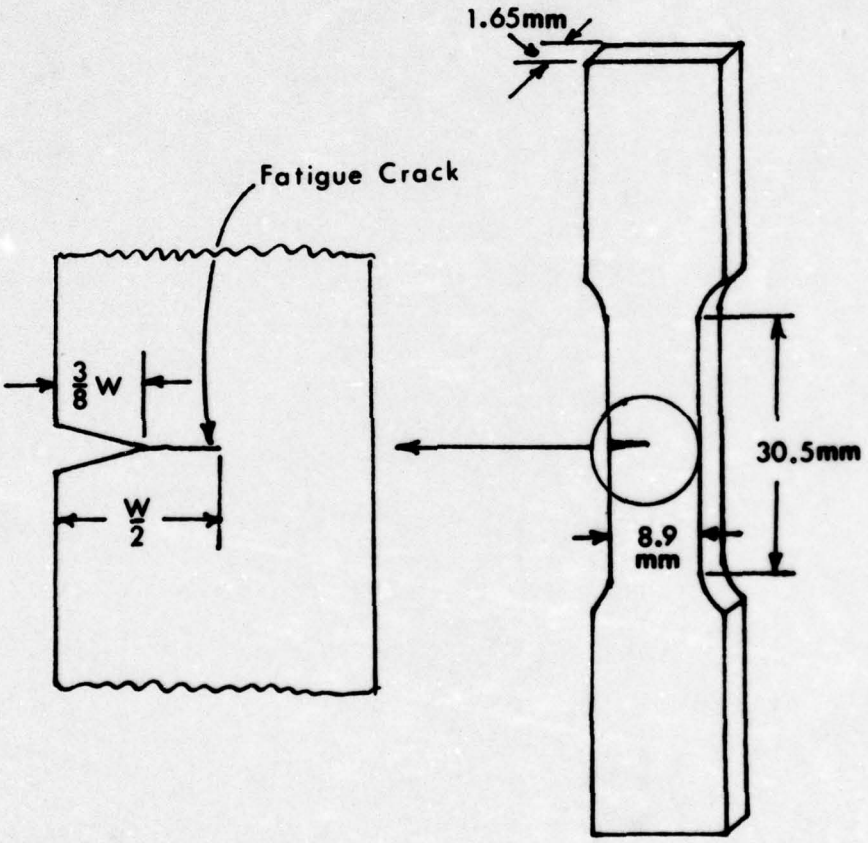

Fig. 1. A schematical drawing of the fracture toughness sample configuration used in this study.

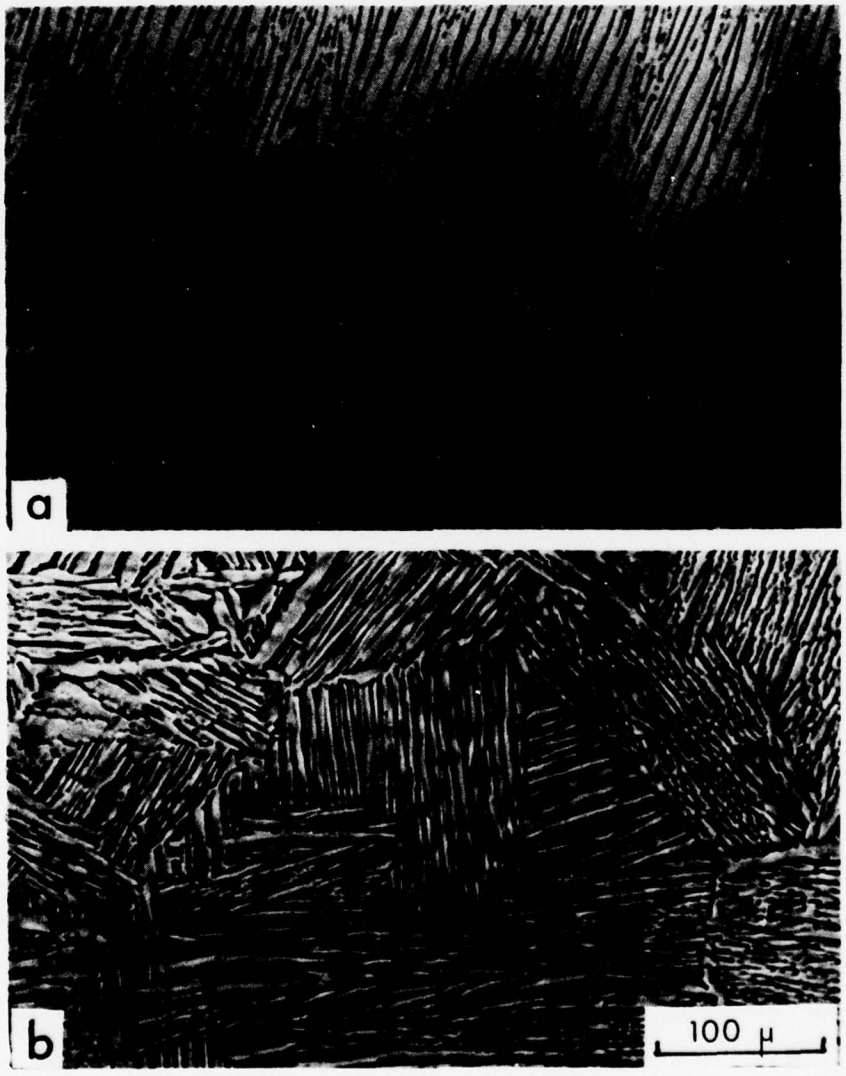

Fig. 2. Optical micrographs illustrating the Widmanstatten microstructure in: (a) a single colony and (b) a multi-colony specimen of the Ti-8Al-1Mo-1V alloy.

followed by a furnace cool (∿200°C/hr) to 730°C, water-quenched and followed by a vacuum anneal at 760°C for two hours and a helium quench. The microstructure, which is shown in Fig. 2b, had a colony size of about 0.27mm. The specimen preparation procedure was similar to that used for the single colonies with the test specimen conforming to the geometry shown in Fig. 1.

The fracture toughness parameters K, the stress intensity factor, and G, the strain energy release rate, were calculated taking into account the mode of crack opening; see Appendix I. A finite width correction factor Y for an edge cracked sample with a mode I crack[18] was incorporated as was the very small correction for the presence of the notch $f(\phi)$, which is tabulated for mode I and II cracks.[19] We assume that the appropriate correction factors for mode II and III cracks are approximately the same as that for mode I so that for the i^{th} mode of opening: $K_i = Y \cdot f(\phi) \cdot \alpha\sqrt{a}$.

It should be recalled that for a mixed mode crack in plane stress, the total strain energy release rate is given simply by the sum of the mode I, II, and III components, which in terms of the values of K_i for mode I, II and III openings for plane stress is:

$$G = \frac{1}{E}\left(K_I^2 + K_{II}^2 + \frac{1}{1+\nu} K_{III}^2\right), \qquad (1)$$

where E is the Youngs modulus and ν is Poisson's ratio. It should be noted that, based on the appropriate elastic constants,[20,21] the elastic anisotropy of α Ti is only 1.33 while the retained β is 1.69. Thus we assume the validity of the relations for the crack-tip stresses based on linear fracture mechanics assuming isotropic elasticity. Also the geometry of the specimens were such that specimen shape corrections discussed by Bowen[5] could be ignored.

The experimental determination of the fracture toughness parameters were made by recording load-displacement curves generated by tests performed at a crosshead speed of 2.5mm/min. During loading, the crack was observed through a traveling

microscope at 10X, and the load of the onset of crack extension (≃ .02mm) was recorded. The development of the plastic zone at the crack tip was observed by interrupting some of the tests and applying replica tape to the crack tip region.

The macroscopic fracture planes as well as (where possible) the active slip and twinning planes were determined by the two surface trace analysis knowing the crystallographic orientation of the colony. Features of the fracture surface were studied using a JEOL JSM-U3 scanning electron microscope.

RESULTS

Fatigue crack propagation across individual Widmanstatten colonies in α-β Ti alloys is known to occur in a Stage I manner on macroscopic planes often inclined to the stress axis.[11,22] Fig. 3 shows the α-phase orientation of the fatigue crack plane. As observed by Wojcik,[14] Fig. 3b shows that there is a strong tendency for fatigue crack propagation to occur on or near (<10°) to the (0001) plane of the α-phase. Given the orientations of the specimens in Fig. 3a, samples 4, 6, 7, and 9 exhibit predominantly mode I cracking with the crack plane being nearly perpendicular to the stress axis (see Table I). Two surface trace analysis of the crack-tip region (the orientation of the trace on the edge face of the specimen is first assumed and then checked after the specimen is broken) indicates (0001) slip as well as twinning on unidentifiable systems occur in these samples where cracking occurs on the (0001) plane in a mode I manner. However, when fatigue crack propagation occurs in a mixed mode manner, such as in sample 1, the crack-tip plasticity is characterized by slip on a single system only, and this is identifiable (0001) slip. It should be noted that the fatigue cracking occurs under conditions of plane strain.

A general feature of the fracture toughness tests was that initial crack extension occurred under conditions of rising load with crack growth beginning at $\sigma < \frac{2}{3}\sigma_y$. Thus a substantial increase in load occurred between the point of observable crack extension ($\Delta a \simeq .02$mm) and the point of load instability. The

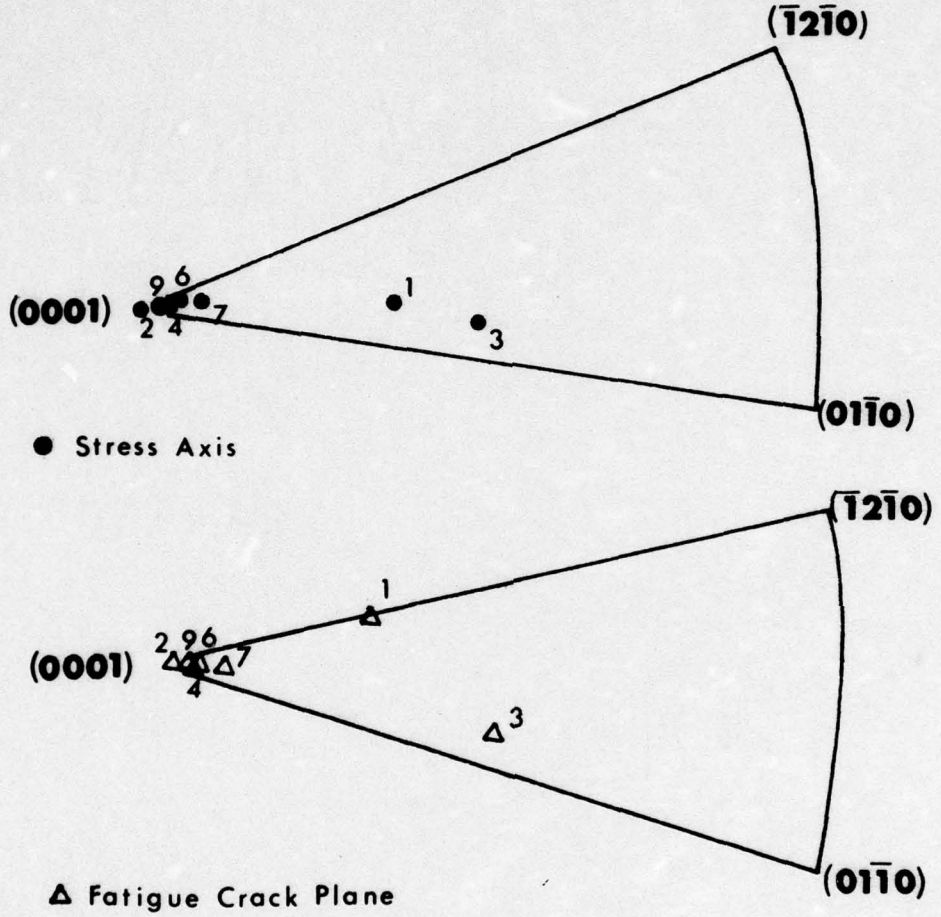

Fig. 3. Standard stereograph projections indicating: (a) the orientations of the stress axis of the specimens and (b) the orientations of the fatigue pre-crack planes. All orientations are those of the hcp α phase in the alloy.

TABLE I. The characterization of the fracture planes, associated crack-tip plasticity and the fracture toughness for individual α-β colonies of the Ti-8Aℓ-1Mo-1V Alloy.

Sample	Mode of Precrack	Fracture Planes*	Crack-tip Plasticity†		at Δa ≃ .02mm		at max. load ≃ G_c^m(MPa-m)
			Deformation	Slip/Twin Planes†	K(MPa$\sqrt{m}$)	G(MPa-m)	
3	I	∿$(10\bar{1}1)$ ∿$(\bar{1}101$	S + T	(0001) S - F $\{10\bar{1}1\}$ S + twins	K_{IC} = 83	6.3	8.4
4	I	∿$(10\bar{1}2)$	S + T	(0001) S - F $\{10\bar{1}2\}$ T + other T	K_{IC} = 77	4.0	7.0
6	I	$(\bar{1}012)$	S + T	(0001) S - F $\{10\bar{1}2\}$ T	K_{IC} = 79	4.2	7.2
7	I	$(10\bar{1}2)$	S + T	(0001) S - F $\{10\bar{1}2\}$ T + other T	K_{IC} = 78	4.2	5.0
9	I	$(\bar{1}012)$ $(10\bar{1}2)$	S + T	(0001) S - F $\{10\bar{1}2\}$ T + other T	K_{IC} = 77	4.0	7.2
1	I, II + III	(0001)	S	(0001) S - C $\{10\bar{1}1\}$ S	K_{IC} = 49 K_{IC} = 19	2.3	3.1
Poly-Xtal	I	-	S + T	-	K_{IC} = 90	6.8	9.6

*As the fracture planes are not crystallographically flat, local deviations of $\lesssim \pm 10°$ can occur.

†S denotes slip, T denotes twinning, C denotes coarse, and F denotes fine.

results of the fracture toughness tests of the individual colonies as well as the polycrystalline sheet specimens is shown in Table I. The toughness values at initial crack extension (G_c) may be grouped roughly into three categories according to the magnitudes of G_c: (a) sample 3 ($G_c = 6.3 \times 10^{-2}$ MPa-m) exhibits high toughness nearly equal to that of polycrystalline specimens, (b) most of the samples exhibit an intermediate toughness of about $3.9 \times 10^{-2} - 4.2 \times 10^{-2}$ MPa-m, and (c) sample 1 ($G_c = 2.3 \times 10^{-2}$ MPa-m) exhibits clearly inferior fracture resistance.

Substantial crack extension ($\Delta a \simeq \approx .08$mm) occurs prior to the maximum load. As will be discussed later, crack extension both prior to and after maximum load occurs on planes inclined to the thickness as well as the width of the specimens, often sequentially on more than one microscopic plane. For all of the samples, this means that the fast fracture crack plane differs from the fatigue crack plane, and the crack assumes a complex, three-dimensional, dog-leg appearance with the onset of subcritical crack growth. Thus, any calculation of the toughness values at maximum load must be viewed as rough estimate, expecially since the stress at maximum load exceeds $(2/3)\sigma_y$ for most of the colony specimens. Such data in the form of the critical strain energy release rate at maximum load (G_c^m) is included in Table I. Although this data must be viewed with reservation, it is consistent with the behavior at initial crack extension in that sample 1 exhibits significantly less fracture resistance than do the other samples.

Crack growth induced by the tensile stress occurs on planes inclined through the thickness at angles of 55-65° and across the width at angles of 30-60°, depending on the specimen. Considerable surface relief and through thickness deformation accompanies such cracking. Two surface trace analysis indicates that the macroscopic fracture planes of individual colony specimens are generally within 5° of certain crystallographic planes in the α-phase, namely either the basal or pyramidal planes; these results are also shown in Table I. It should be

noted that the macroscopic tensile fracture plane differs from the fatigue crack plane in all of the samples, although the tensile fracture plane is close (∿10°) to the fatigue plane in sample 1.

Table I also describes the crack-tip plasticity in terms of slip and/or twinning in the α-phase. All samples possessed at least one active deformation system on a plane inclined through the specimen thickness. The samples which possessed pre-cracks of mode I type exhibit both slip and twinning (on planes inclined through the thickness) at the crack tip under subsequent tensile loading. However, only slip was observed in those specimens exhibiting mixed mode cracking and in which the basal plane of the α-phase is inclined to the stress axis. Among the samples, there is also a distinction to be made in the homogeneity of slip. High toughness is associated with relatively fine, multiple slip and twinning (see Fig. 4a) while coarse slip bands are observed at the crack-tip and along the fracture surface of specimens with low toughness (see Fig. 4b).

The appearance of the fracture surface is very dependent on colony orientation. Most of the specimens do not show a significant difference between the regions at subcritical crack growth and of rapid crack extension at maximum load. Unlike the behavior of textured Ti-6Aℓ-4V, there is no evidence of a stretch zone in any of the samples. This difference may be related to the difference in state of stress (plane stress in our case) and to the single crystal nature of the deformation in the present case. Where twinning occurs as a mode of crack-tip plasticity, fractography indicates a mixture of dimpled fracture and some regions of fracture associated with or close to the twin-matrix interface (see lower right portion of Fig. 5). The incidence of fracture related to the twin-matrix interfaces is more prevalent in samples of intermediate toughness than in samples of high toughness.

Typical fracture surfaces of the two samples (1 and 3) exhibiting the lowest and highest fracture resistance are shown in Fig. 6. Both samples fail by

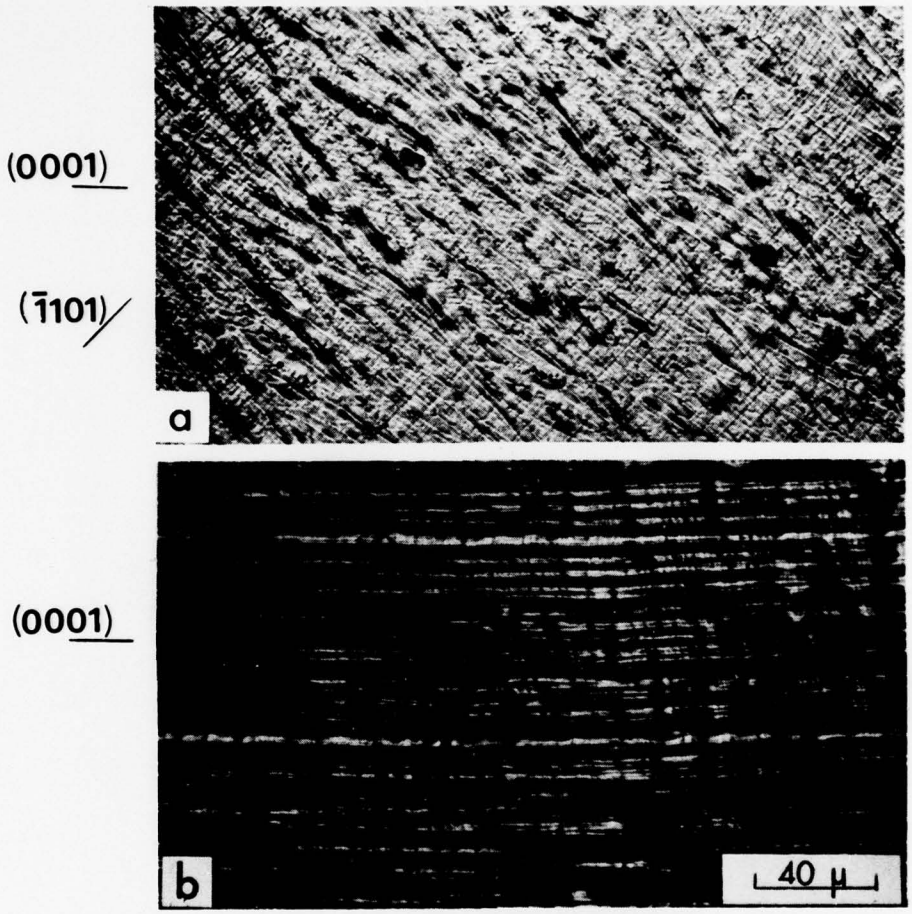

Fig. 4. Slip morphology near the fracture surface of specimens exhibiting: (a) high fracture toughness and (b) low fracture toughness.

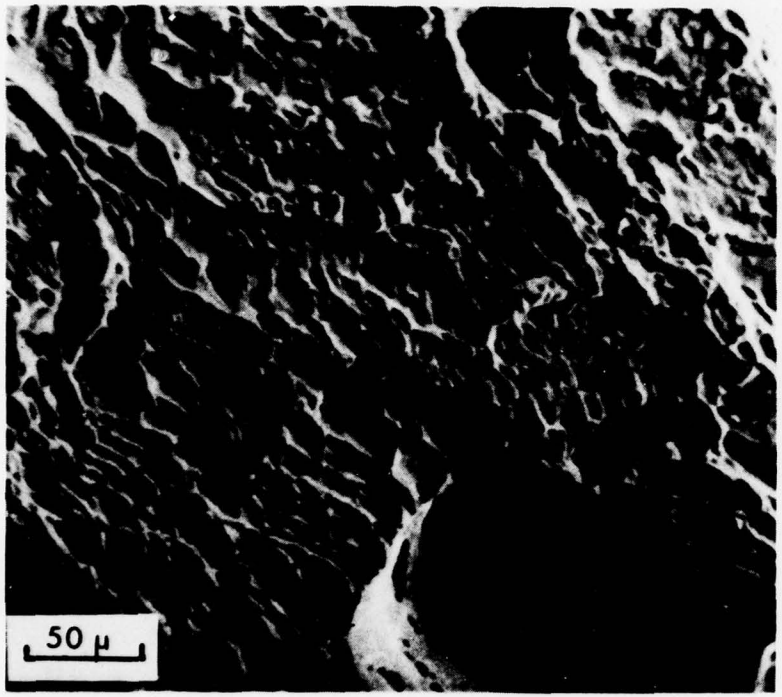

Fig. 5. Electron micrograph showing the fracture surface of sample--(intermediate toughness). The region in the lower right corner is fracture along a twin-matrix interface.

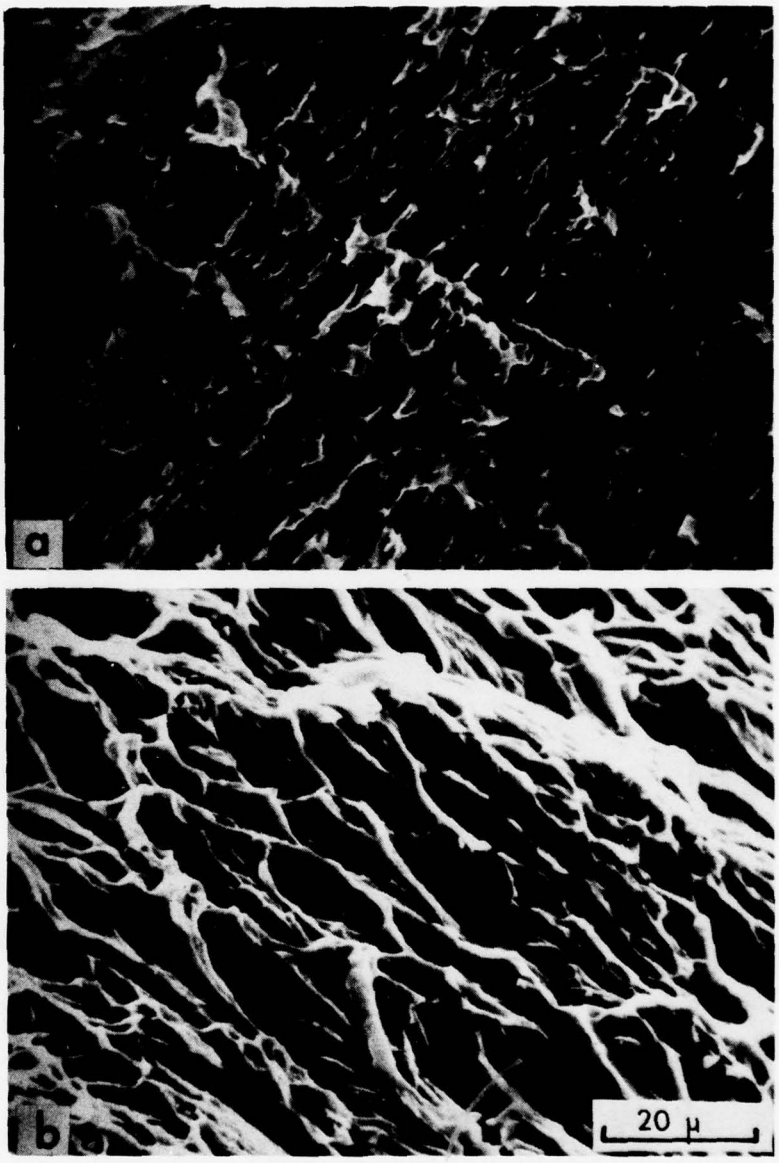

Fig. 6. Electron micrographs contrasting the fracture surfaces of: (a) sample 1 (low toughness) and (b) sample 3 (high toughness).

microvoid coalescence but the dimple size and morphology differs. The low toughness sample (no. 1) in Fig. 6a, is associated here with microvoids which are larger and more shallow and elongated in comparison to those found on the fracture surface of a specimen (sample 3) in Fig. 6b, which possesses high toughness. The geometric alignment of the dimples and the general features in Fig. 6a is remindful of the "troughs" observed elsewhere,[6] and are probably associated with the presence of the β-phase. Such troughs are not common, and it should be noted that in most samples the presence of the β-phase appears to have little direct influence on the appearance of the fracture surface. The size and the morphology of the dimples does not appear directly related to the plate-like shape and spacing of the β lamellae in most samples.

The polycrystalline colony samples exhibit a significant amount of fracture along inter-colony boundaries. Such fracture behavior and the general fractographic features of these samples are similar to those of other α-β Ti alloys with Widmanstatten microstructures.[11,12,14]

DISCUSSION

The tensile fracture behavior of pre-cracked, individual Widmanstatten colonies is characterized by certain features: (a) crack propagation occurs on planes inclined both across the width and through the thickness of the specimen; (b) crack-tip plasticity always involves through-thickness deformation in the form of slip and, in some cases twinning; (c) the fracture toughness both at initial crack growth and at maximum load depends on colony orientation with low toughness being associated with coarse, planar slip in the α-phase; and (d) with some exceptions, fractography indicates relatively little direct influence of the β phase on the differences in fracture toughness among the samples. These observations indicate the following basis of analysis.

Given the thickness of the specimens (1.65mm), the toughness ($\sim$80 MPa$\sqrt{\text{in}}$) and the yield strength ($\simeq$700 MPa), one would expect a plastic zone size ($\simeq$2mm)

equal to the specimen thickness. Thus, tensile fracture should occur under conditions of plane stress. This is fully consistent with the observations summarized above of the shear-type plane of cracking as well as the through-thickness deformation present in all of the samples. Thus, we conclude that tensile crack propagation occurs under plane stress.

It is well established that plane stress crack propagation usually occurs on the plane of maximum shear stress. For a plastically isotropic material, this corresponds to plane inclined across the thickness of the specimen at $\sim 45°$ but <u>not</u> inclined to the specimen width. Such behavior is observed in the present study for the polycrystalline material but <u>not</u> for the single colonies where the crack plane is inclined across the width as well as the thickness. An obvious possibility is that the anisotropic deformation behavior of the individual colony controls the fracture path and therefore influences the fracture toughness of a colony. Experimental observations indicate fracture occurs near crystallographic slip or twinning planes. Thus, it seems likely that fracture occurs on that crystallographic deformation plane which experiences the maximum shear stress under conditions of plane stress. The following analysis examines this possibility as well as the resulting implications with regard to the relative magnitude of the fracture toughness of an individual colony.

The basis for analyzing the tensile fracture behavior of the pre-cracked α-β colonies is to determine the relative magnitude of the shear stresses acting on selected crystallographic planes and directions subject to the condition that the macroscopic stress resulting from the stress field of a crack loaded under conditions of plane stress is a maximum. The crystallographic planes and directions analyzed are those slip, twinning, or fracture planes observed to be active in the α-phase as well as those which should have high shear stresses. The crack-tip stress field used in the analysis is that for the fatigue pre-crack, which is planar, and whose geometry is reasonably well known. Thus this analysis should

apply relatively well to the initiation and sub-critical crack growth stage upon tensile loading. At maximum load, the crack already has a dog-leg appearance, the stress field will be altered somewhat, and the analysis will only be a rough approximate indication of the distribution of shear stresses on various slip/twinning systems.

For the maximum macroscopic shear stress, we assume the Tresca condition since this physically locates the plane of maximum shear stress which, in the case of polycrystalline material, usually is the fracture plane in plane stress. If σ_1, σ_2, and σ_3 are the principal stresses, then:

$$\tau_{max} = \frac{\sigma_1 - \sigma_3}{2} \tag{2}$$

The application of eqn. 2 is straightforward for a mode I crack,[23] which characterizes the pre-cracks in the polycrystalline samples and most of the single colony specimens tested (see Table I). The principal stress components for a mode I crack are:[23]

$$\sigma_1 = \frac{K_I}{\sqrt{2\pi r}} \cos\frac{\theta}{2}\left(1 + \sin\frac{\theta}{2}\right)$$

$$\sigma_2 = \frac{K_I}{\sqrt{2\pi r}} \cos\frac{\theta}{2}\left(1 - \sin\frac{\theta}{2}\right) \tag{3}$$

$$\sigma_3 = 0,$$

where K_I is the mode I stress intensity factor, θ is the angle of inclination at the crack tip measured from the crack plane, and r is the distance from the crack tip at an angle θ. For the polycrystalline material, the maximum, macroscopic shear stress τ_{max} occurs when σ_1 is maximized (since $\tau_{max} = \frac{1}{2}(\sigma_1 - \sigma_3) = \frac{1}{2}\sigma_1$). Solving $(\partial\sigma_1/\partial\sigma)_r = 0$, we obtain the value of θ at which τ_{max} occurs, which is $\theta_m = 60°$. At this value of θ, $\tau_{max} = 0.65\ K_I/\sqrt{2\pi r}$ and acts on a plane inclined 45° across the thickness of the sample but 90° across the width. That cracking occurs in polycrystalline material on such a plane is consistent with the concept that plane stress crack propagation is a shear fracture process, possibly because

of a critical shear strain criteria for local fracture.

For a single colony there is a conflict between what the macroscopic stress field dictates and what the crystallography of the microscopic slip or twinning system will permit. At the crack-tip, the maximum macroscopic shear stress still occurs at $\theta_m = 60°$. However, there are no crystallographic slip or twinning planes which coincide with this maximum macroscopic shear stress plane. Thus the crystallography of slip and twinning must be accommodated if a maximum shear stress criteria is to be applied to the plane stress fracture of single colonies. The shear stress τ on a given plane with a normal $\vec{n}$ and a shear displacement direction $\vec{b}$ is:[24]

$$\tau = \frac{1}{b} \vec{b} \cdot \vec{\vec{\sigma}} \cdot \vec{n}, \tag{4}$$

where $\vec{\vec{\sigma}}$ is the stress tensor describing the state of stress near the crack-tip, given a linear elastic material. These stress components are given in the appendix for the general case of a mixed mode crack.

Since σ depends on the value of the angle θ with respect to the crack plane, the question becomes what value of θ (in eqn. 3) is appropriate for a maximum shear stress criteria. There are two likely possibilities: first, θ has that value (θ_{max}) at which the macroscopic shear stress τ_{max} is a maximum according to the Tresca condition (eqn. 2) and, second, θ is determined by the maximum value τ_{max}^{micro} of the "microscopic" shear stress τ (eqn. 4) on a through-thickness slip/twinning plane ahead of the crack; i.e., $-90° \leq \theta \leq 90°$. In the case of sample 1 which has a mixed mode I, II, and III pre-crack, the magnitude of θ_{max} can be obtained by maximizing eqn.[3] numerically as σ_1, σ_2, and σ_3 are determined as a function of θ. The values of the principal stresses for the given three dimensional state of stress are solved using conventional techniques.[25]

Table II shows the results of the calculations of the shear stresses on various through-thickness slip or twinning systems at the tip of the fatigue pre-crack, using either the macroscopic or microscopic shear stress criteria. A comparison

TABLE II. The relative magnitudes of the shear stress τ (in units of $\sigma\sqrt{a/2r}$) acting on most highly stressed slip or twinning systems subject to a condition of maximum, macroscopic shear stress at the tip of the precrack under plane stress loading. The angle θ_{max} refers to the angle at which $(\sigma_1-\sigma_3)/2$ is a maximum.

Sample	Slip or Twinning System	Macro. Criteria		Micro. Criteria		G_{crit} [MPa-m]
		θ_{max}	τ @ θ_{max}	τ_{max}^{micro}	θ	
3	$(\bar{1}101)[11\bar{2}0]$*	60°	.57	.60	74°	6.3
	$(10\bar{1}1)[12\bar{1}0]$*		.53	.55	72°	
	$(0001)[11\bar{2}0]$		.35	.40	-76°	
	$(10\bar{1}2)[\bar{1}011]$		.47	.64	26°	
	$(\bar{1}100)[11\bar{2}0]$		.32	.33	66°	
4.6 7.9	$(\bar{1}012)[10\bar{1}1]$*	60°	.59	.59	64°	4.1
	$(10\bar{1}2)[\bar{1}011]$*		.59	.59	64°	
	$(10\bar{1}0)[\bar{1}2\bar{1}0]$		.19	.43	4°	
	$(01\bar{1}2)[01\bar{1}1]$		.43	.46	-72°	
	$(0001)[11\bar{2}0]$		0	.31	90°	
1	$(0001)[11\bar{2}0]$*	42°	.43	.49	+22°	2.3
	$(1\bar{1}01)[11\bar{2}0]$		.34	.50	+ 2°	
	$(\bar{1}100)[11\bar{2}0]$		.16	.45	-14°	
	$(1\bar{1}02)[\bar{1}101]$		.32	.35	-90°	
Poly-crystal-line	Slip + Twinning	60°	-	-	-	6.8

*Approximate macroscopic fracture plane.

between the slip systems observed (Table I) and those predicted to be highly stressed (Table II) supports the validity of these calculations. An examination of the relative values of the shear stresses on the various crystallographic systems indicates that the macroscopic planes of tensile fracture are close to those slip or twinning planes which experience the largest shear stress under conditions of maximum macroscopic shear stress. In contrast, there does not appear to be a correlation in Table II between the observed fracture plane and the maximum microscopic shear stress on a slip/twinning system in the vicinity of the crack-tip. Thus we conclude that the plane stress tensile crack growth of both poly-colony and individual colony material of this α-β Ti alloy occurs on or near planes of maximum macroscopic shear stress subject to the constraints in the colony material that fracture occurs on or near a crystallographic slip or twinning system. Given the presence of microvoids on most of the fracture surfaces, the crack can be viewed as following a path of maximum void concentration, probably a result of the concentration of shear strain.[23,26] As indicated previously, the above calculations should apply directly to the subcritical crack growth regime, and roughly to the onset of unstable cracking. The absence of any substantial change in fracture appearance and crack planes between the slow and unstable crack growth stages also indicates that the above "maximum macroscopic shear stress" criteria applies to both crack stages.

The calculated shear stresses in Table II also give an indication why tensile fracture is accompanied by multiple slip/twinning in some cases but not in others. If at the point of tensile crack advance the distribution of shear stresses is such that several deformation systems are all highly stressed, then multiple slip/twinning should occur. This seems to be the case if one compares the calculated τ values in Table II with the observed slip systems in Table I. However, care must be taken in such an interpretation, since the monotonic compressive yield behavior of individual α+β colonies shows that there is no well-defined

critical resolved shear stress for activating slip on a given system in the lamellar, Widmanstatten microstructure.[27] Simply because a slip system is highly stressed does not mean that it will be active on a macroscopic scale across α-β lamellae.

The question of the relative toughness of the individual colonies remains. The experimental results, such as Fig. 4, indicate that high fracture toughness is associated with multiple slip and twinning which results in relatively homogeneous deformation. On the other hand, low toughness occurs when slip is confined primarily to the basal plane and coarse, comparatively inhomogeneous slip bands occur (compare Figs. 4a and 4b). An obvious reason for the correlation between toughness and multiple slip and twinning is that concurrent slip and twinning on several systems causes high work hardening, which is known to enhance toughness,[28] probably because of a better resistance to strain localization.[29] Once strain localization occurs and crack propagation along a "primary" slip band co-planar with the crack takes place, plastic relaxation <u>normal</u> to the slip band is hindered. This is especially true in the case of sample 1 which fails along the basal plane. The constraints of hcp crystallography make plastic extension along the C axis very difficult, and displacements along the C axis remain elastic to large stresses. In the limit, with the slip vector being confined to the "primary" slip plane, an elastic-plastic state of stress occurs with the shear stresses in the slip plane being relaxed but the normal stresses remaining elastic until secondary slip (with a slip vector inclined to the primary slip plane) is activated close to the crack tip. Such a model for crack propagation has been analyzed by Koss and Chan,[30] and the results indicate a combination of large hydrostatic or normal stresses near the crack-tip combined with intense shear. Thus, a critical stress and strain fracture criteria[23,26] would be satisfied at a smaller external stress when crack-tip deformation is confined to narrow, inhomogeneous basal slip bands co-planar with the crack. In contrast, when slip is homogeneous and crack extension

occurs along non-basal planes, plastic relaxation of the normal stresses is relatively easy resulting in smaller normal stresses. The more uniform nature of the deformation also means that it is more difficult to achieve the critical shear strain criteria. The result is that toughness increases when slip is homogeneous and non-basal cracking is involved. This concept should apply to plane strain as well as plane stress fracture behavior.

SUMMARY

The plane stress fracture toughness of individual Widmanstatten colonies of a near-α, α-β Ti alloy can be related to the deformation behavior of the crack-tip. The crack-tip plasticity is characterized both by experimental observations and by calculations of the distribution of shear stresses on selected slip or twinning systems. As indicated by polycrystalline behavior, fracture of single colonies obeys a maximum, macroscopic shear stress criteria subject to the constraints of the crystallography of slip or twinning in that colony. High fracture toughness is associated with multiple slip and fine twinning at the crack-tip and with the avoidance of fracture along or near twin-matrix or α-β interfaces. Multiple slip and twinning can cause high toughness through the relatively high work hardening and the fine and homogeneous crack-tip deformation behavior which results. The localization of strain into coarse inhomogeneous basal slip bands co-planar with a crack results in an elastic-plastic stress state with large normal stresses accompanying intense shear, and inferior fracture toughness results. The fracture behavior of the individual colonies is such that the role of the β phase may be viewed as primarily affecting deformation in the α-phase; this is probably not true with polycrystalline material where intercolony fracture also occurs.

ACKNOWLEDGEMENT

The authors wish to thank the Titanium Metals Corporation of America for supplying the material. This research was supported by the Office of Naval Research under Contract No. N00014-76-C-0037.

References

1. F. R. Larsen and A. Zarkades, MCIC Rep. 74-20 (1974).

2. A. Zarkades and F. R. Larsen in Titanium Science and Technology, Vol. 2, p. 1321. Plenum Press, New York (1973).

3. H. W. Rosenberg and W. M. Parris, ASTM STP 556, 26 (1974).

4. M. J. Harrigan, A. W. Sommer, P. G. Riemers, and G. A. Alers, in Titanium Science and Technology, Vol. 2, p. 1297. Plenum Press, New York (1973).

5. A. W. Bowen, Acta Met., 26, 1423 (1978).

6. R. M. Tchorzewski and W. B. Hutchinson, Met. Trans., 9A, 1113 (1978).

7. W. W. Gerberich and G. S. Baker in Applications-related Phenomena in Titanium Alloys, ASTM STP 432, p. 80. ASTM, Philadelphia, 1968.

8. R. E. Curtis and W. F. Spurr, Trans. ASM 61, 115 (1968).

9. M. A. Greenfield and H. Margolin, Met. Trans., 3, 2649 (1972).

10. D. H. Rogers, in Titanium Science and Technology, Vol. 2, p. 1719. Plenum Press, New York, (1973).

11. D. Eylon, J. A. Hall, C. M. Pierce, and D. L. Ruckle, Met. Trans., 7A, 1817 (1976).

12. J. C. Chesnutt, C. G. Rhodes, J. C. Williams in Fractography-Microscopic Cracking Processes, ASTM STP 600, p. 99. ASTM, Philadelphia, 1976.

13. N. L. Richards and J. T. Barnby, Mat'l. Sci. and Eng., 26, 221 (1976).

14. I. W. Hall and C. Hammond, Mat'l. Sci. and Eng., 32, 241 (1978).

15. C. C. Wojcik, M.S. Thesis, Michigan Technological University, 1977.

16. M. J. Blackburn, Trans. ASM, 59, 694 (1966).

17. C. G. Rhodes and J. C. Williams, Met. Trans., 6A, 1670 (1975).

18. W. F. Brown and J.E. Srawley in Plane Strain Crack Toughness Testing of High Strength Metallic Materials, ASTM STP 410, p. 114. ASTM, Philadelphia, 1965.

19. B. Gross and A. Mendelson, J. Frac. Mech., 8, 267 (1972).

20. E. S. Fisher and C. J. Renken, Phys. Rev. 135, A482 (1964).

21. L. Graham and G. Alers, in article by E. S. Fisher in The Physics of Solid Solution Strengthening, p. 204. Plenum Press, New York, 1975.

22. D. Schechtman and D. Eylon, Met. Trans., 9A, 1018 (1978).

23. D. Broek, Elementary Engineering Fracture Mechanics, Chapts. 2, 3, 5, 8, and 11. Noordhoff Int. Publishing, Leydon, Netherlands, 1974.

24. M. O. Peach and J. S. Koehler, Phys. Rev., 80, 436 (1950).

25. A. C. Ugural and S. F. Fenster, Advanced Strength and Applied Elasticity, p. 17. American Elsevier, New York, 1975.

26. F. A. McClintock and G. R. Irwin, in Fracture Toughness Testing and its Applications, ASTM STP 410, p. 84. ASTM, Philadelphia, 1965.

27. K. Chan and D. A. Koss, unpublished results.

28. G. T. Hahn and A. R. Rosenfield in Applications-Related Phenomena in Titanium Alloys, ASTM STP 432, p. 5. ASTM, Philadelphia, 1968.

29. E. Smith, T. S. Cook, and C. Rau, in Fracture 1977, Vol. 1, p. 215. Univ. of Waterloo Press, Canada, 1977.

30. D. A. Koss and K. Chan, unpublished results.

APPENDIX I

Determination of the Stress Components for a Mode I, II and III Crack

Figure I-A shows a mixed-mode I, II and III crack inclined to the stress axis Y in a manner such that Y makes angles η, ψ and ξ with the X', Y' and Z' axes of the crack respectively. Let σ be the tensile stress in the Y direction, then the stress transformation of σ into the X'Y'Z' coordinate system would be:

$$\begin{aligned} \sigma_{y'y} &= \sigma \cos^2 \psi \\ \sigma_{y'x'} &= \sigma \cos \psi \cos \eta \\ \sigma_{y'z'} &= \sigma \cos \psi \cos \xi \end{aligned} \qquad \text{Eq. (A1)}$$

Hence (23):

$$\begin{aligned} K_I &= \sigma \cos^2\psi \sqrt{\pi a} \\ K_{II} &= \sigma \cos \psi \cos \eta \sqrt{\pi a} \\ K_{III} &= \sigma \cos \psi \cos \xi \sqrt{\pi a} \end{aligned} \qquad \text{Eq. (A2)}$$

The stress field for the mixed-mode (I, II and III) crack under plane stress is (23):

$$\sigma_{x'x'} = \frac{\sigma\sqrt{\pi a}}{\sqrt{2\pi r}} \left\{\cos^2\psi\cos\frac{\theta}{2}\left(1-\sin\frac{\theta}{2}\sin\frac{3\theta}{2}\right) - \cos\eta\cos\psi\left(2+\cos\frac{\theta}{2}\cos\frac{3\theta}{2}\right)\sin\left(\frac{\theta}{2}\right)\right\}$$

$$\sigma_{y'y'} = \frac{\sigma\sqrt{\pi a}}{\sqrt{2\pi r}} \left\{\cos^2\psi\cos\frac{\theta}{2}\left(1+\sin\frac{\theta}{2}\sin\frac{3\theta}{2}\right) + \cos\eta\cos\psi\left(\sin\frac{\theta}{2}\cos\frac{\theta}{2}\cos\frac{3\theta}{2}\right)\right\}$$

$$\sigma_{z'z'} = 0 \qquad \text{Eq. (A3)}$$

$$\sigma_{x'y'} = \frac{\sigma\sqrt{\pi a}}{\sqrt{2\pi r}} \left\{\cos^2\psi\sin\frac{\theta}{2}\cos\frac{\theta}{2}\cos\frac{3\theta}{2} + \cos\eta\cos\psi\cos\frac{\theta}{2}\left(1-\sin\frac{\theta}{2}\sin\frac{3\theta}{2}\right)\right\}$$

and $\sigma_{x'z'} = -\frac{\sigma\sqrt{\pi a}}{\sqrt{2\pi r}} \left\{\cos\psi\cos\xi\sin\frac{\theta}{2}\right\}$ and $\sigma_{y'z'} = \frac{\sigma\sqrt{\pi a}}{\sqrt{2\pi r}} \left\{\cos\psi\cos\xi\cos\frac{\theta}{2}\right\}$

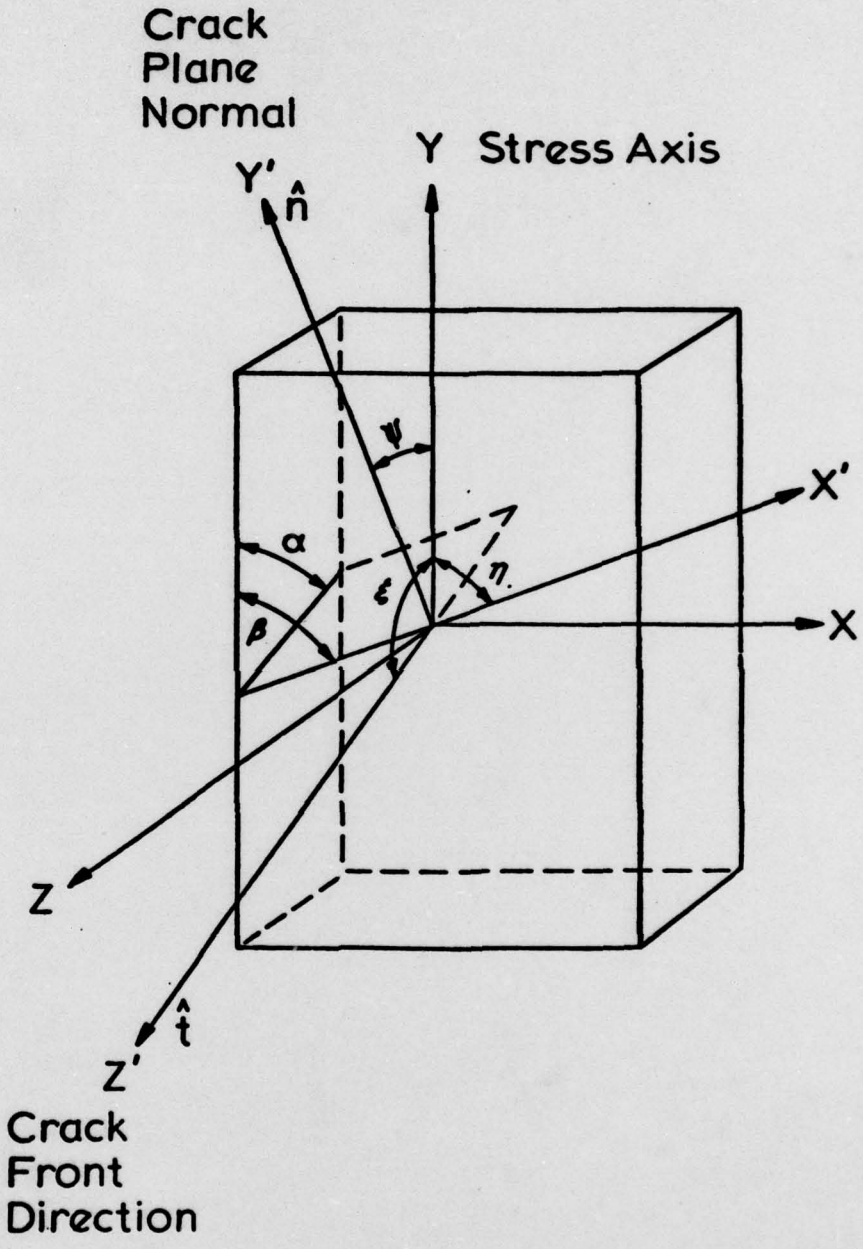

Fig. IA. The configuration of a mixed-mode crack with mode I, II, and III components.

SECURITY CLASSIFICATION OF THIS PAGE (When Data Entered)

(14) TR-

REPORT DOCUMENTATION PAGE

READ INSTRUCTIONS BEFORE COMPLETING FORM

1. REPORT NUMBER: No. 9

2. GOVT ACCESSION NO.

3. RECIPIENT'S CATALOG NUMBER

(9) Technical rept.

4. TITLE (and Subtitle)

(6) FRACTURE TOUGHNESS OF WIDMANSTATTEN COLONIES OF AN ALPHA-BETA TITANIUM ALLOY,

5. TYPE OF REPORT & PERIOD COVERED

6. PERFORMING ORG. REPORT NUMBER

7. AUTHOR(s)

(10) K. S. Chan and D. A. Koss

8. CONTRACT OR GRANT NUMBER(s)

(15) N00014-76-C-0037

9. PERFORMING ORGANIZATION NAME AND ADDRESS

Department of Metallurgical Engineering
Michigan Technological University
Houghton, MI 49931

10. PROGRAM ELEMENT, PROJECT, TASK AREA & WORK UNIT NUMBERS

11. CONTROLLING OFFICE NAME AND ADDRESS

(11) Metallurgy Program, Office of Naval Research
800 North Quincy St.
Arlington, VA 22217

12. REPORT DATE

Jun[illegible] 1979

13. NUMBER OF PAGES

28

14. MONITORING AGENCY NAME & ADDRESS (if different from Controlling Office)

(12) 39p.

15. SECURITY CLASS. (of this report)

Unclassified

15a. DECLASSIFICATION/DOWNGRADING SCHEDULE

16. DISTRIBUTION STATEMENT (of this Report)

Distribution of this document is unlimited.

17. DISTRIBUTION STATEMENT (of the abstract entered in Block 20, if different from Report)

18. SUPPLEMENTARY NOTES

19. KEY WORDS (Continue on reverse side if necessary and identify by block number)

Fracture, fracture toughness, α-β Ti alloy, individual colonies, inhomogeneous slip

20. ABSTRACT (Continue on reverse side if necessary and identify by block number)

The fracture toughness behavior of individual α-β Widmanstatten colonies of the Ti-8Al-1Mo-1V alloy in the form of sheet has been investigated. Crack extension occurs predominantly across the α-β lamellae under conditions of plane stress and on planes which are inclined both to the thickness and the width of specimens. Polycrystalline material has also been examined and is observed to exhibit fracture along a plane inclined through the thickness but not inclined across the width. Crack-tip plasticity in both types of material is (cont'd)

DD FORM 1 JAN 73 1473 EDITION OF 1 NOV 65 IS OBSOLETE
S/N 0102-014-6601

402 311

SECURITY CLASSIFICATION OF THIS PAGE (When Data Entered)

20. Abstract (cont'd)

dominated by through-thickness deformation involving slip and often twinning. In the single colony specimens, the crack-tip plasticity has been characterized experimentally by identifying the active slip/twinning planes and by calculating the distribution of shear stresses on the possible deformation systems, using a maximum, macroscopic shear stress criteria. As suggested by the fracture behavior of the polycrystalline specimens, the macroscopic fracture plane across individual colonies is near that slip or twinning plane which experiences the largest shear stress when the macroscopic shear stress is a maximum. The plane stress fracture toughness of individual colonies depends strongly on colony orientation and also on the nature of the deformation at the crack-tip. High toughness of a colony is associated with multiple slip and twinning and with the absence of low energy fracture along or near interfaces, such as twin boundaries or α-β interfaces. Conversely, slip localization into coarse, inhomogeneous basal slip bands results in the crack extension along such bands and in the lowest fracture toughness observed. Such fracture behavior can be readily understood in terms of an elastic-plastic model for crack advance along slip bands co-planar with a crack.